Available online at www.sciencedirect.com
SCIENCE DIRECT
Journal of Chromatography A, 1092 (2005) 43–54
JOURNAL OF CHROMATOGRAPHY A
www.elsevier.com/locate/chroma

Shortcut method for evaluation and design of a hybrid process for enantioseparations

Malte Kaspereit [a,*], Knut Gedicke [b], Volker Zahn [b], Alan W. Mahoney [c], Andreas Seidel-Morgenstern [a,b]

[a] *Max Planck Institute for Dynamics of Complex Technical Systems, Sandtorstr. 1, D-39106 Magdeburg, Germany*
[b] *Chair for Chemical Process Engineering, Otto-von-Guericke University, D-39106 Magdeburg, Germany*
[c] *Department of Chemical and Process Engineering, University of Sheffield, UK*

Available online 5 March 2005

Abstract

Hybrid processes for enantioseparations have a considerable potential for reducing investment and operational costs. An example is the combination of simulated moving bed (SMB) chromatography and selective crystallisation. However, the design of integrated processes is a difficult task. A shortcut method is presented that can serve as a tool for design and estimation of the potential of such processes. The approach requires only limited experimental data and thus allows for systematic parameter studies. The method is based on the determination of the purity-performance characteristic of the SMB process and rigorous application of mass balances. The use of relative mass fluxes allows derivation of simple algebraic expressions for essential process parameters. The significant potential of combining SMB and crystallisation is demonstrated for the example of the separation of mandelic acid enantiomers.

Keywords: Hybrid processes; Shortcut method; SMB chromatography; Crystallisation; Enantioseparation; Mass balance; Segregation factor; Mandelic acid; TMB; Chirobiotic T

1. Introduction

Enantioseparations are of significant importance for the production of pharmaceuticals. The synthesis of racemates and their subsequent separation remains a fundamental method in the production of pure enantiomers, although there is a high interest in the direct synthesis of enantiomers by chiral catalysis or biocatalysis [1,2]. HPLC is one of the few processes being capable of separating enantiomers, and it is gaining more and more importance [3]. This is due to successful developments of new chiral stationary phases (CSPs) and improvements of their capacity, selectivity, and stability, e.g. [4–7]. Furthermore, the implementation of new concepts like the SMB process led to shorter development and faster production.

However, performance of preparative chromatographic enantioseparations is often poor if compared to "classical" separations like the distillation of bulk chemicals. This is due to the high-purity demands on one hand, and yet limited capacity and selectivity of the available CSPs on the other hand. This combination leads to rather low throughput and high solvent consumption of chromatographic enantioseparations. Furthermore, in preparative scale the investment costs for CSPs can be very high.

One possibility to decrease costs and to improve performance of chromatography-based enantioseparations is the application of hybrid separation processes. Hybrid processes combine two or more different unit operations to resolve a separation task that—in principle—could be managed using only a single process. The implementation of an additional,

* Corresponding author. Tel.: +49 391 6110 282; fax: +49 391 6110 551.
E-mail address: kaspereit@mpi-magdeburg.mpg.de (M. Kaspereit).

0021-9673/$ – see front matter © 2005 Elsevier B.V. All rights reserved.
doi:10.1016/j.chroma.2005.02.043

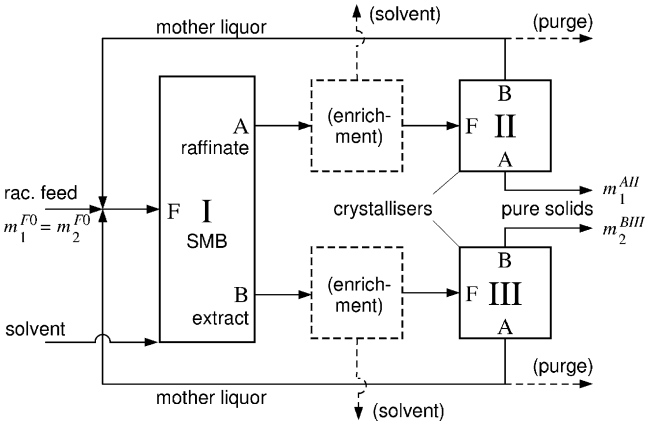

Fig. 1. Continuous SMB chromatography (I) coupled with selective crystallisation units (II and III) for the separation of two enantiomers (1 and 2). The SMB delivers two streams enriched with one of the enantiomers. Pure solid enantiomers are obtained at the outlets of the crystallisers. Dashed lines mark optional removal of solvent for creation of supersaturation.

complementary separation technique can create synergisms, for example, by allowing reduction of purity requirements on the process most strongly limiting performance.[1]

In this work, we will investigate a hybrid process consisting of simulated moving bed (SMB) chromatography and selective crystallisation. This concept might be economically advantageous in comparison to stand-alone separations by SMB, because the chromatography does not have to deliver pure products and therefore its performance parameters (like productivity and solvent consumption) improve [8–11]. Lim et al. [12,13] performed first experimental investigations for the Praziquantel system. Lorenz et al. described the fundamentals of the approach in detail [11]. Ströhlein et al. [14] tried to develop a design method for this process.

Fig. 1 shows a schematic representation of the concept. In this process, an external feed (F0) enters the hybrid process comprising the SMB (unit I) and two crystallisers (units II, III). The SMB feed (inlet FI) is split into two fluxes; the raffinate enriched in the less retained enantiomer 1 (outlet AI), and the extract enriched in the more retained enantiomer 2 (outlet BI), respectively. Pure solid enantiomers are obtained at the respective outlets of the crystallisers, i.e. at AII (enantiomer 1) and BIII (enantiomer 2). A prerequisite is that the enrichment by SMB exceeds the eutectic composition of the system [15]. To achieve high yields, it is necessary to recycle mother liquor from the two crystallisers (outlets BII and AIII) back to the feed of the SMB. Optional purge streams can prevent the accumulation of impurities. A pre-concentration step (e.g. by distillation or membrane processes) is necessary, if concentrations delivered by SMB are too low to perform the crystallisation (denoted as dashed boxes in Fig. 1). For details about this process and its underlying fundamentals, we refer to [11].

[1] In control theory, the term “hybrid” denotes a system containing both continuous and discrete-event components. However, in this work, we will adopt the perspective above.

A general problem one faces when dealing with interconnected processes containing recycles (like the scheme shown in Fig. 1) is that their performance and design are not predictable intuitively. In particular, the determination of optimal values for transition variables between the single units is of great importance. In the case of combined chromatography and crystallisation, obviously the optimal transition composition, i.e. the outlet purity of the chromatographic step, is of major interest.

One possibility to achieve a design for the above process is to perform optimisations of a detailed model. However, because of the nonlinear nature of most preparative chromatographic processes (due to nonlinear adsorption isotherms) and the discrete character of the SMB process (due to column switching) such a model is computationally expensive. Furthermore, in drug development final decisions for process design have to be made at a rather early stage. At this stage often not enough information about the system (solubility equilibria, details regarding the cost function, etc.) is available to allow for a detailed study of complicated processes. To clarify whether it is worthwhile to invest in additional efforts, i.e. to determine all necessary parameters and to perform a detailed study, an efficient method for evaluation appears desirable that uses only a minimum of information.

In this work, we present a strategy for the performance assessment of hybrid separations based on the consequent application of steady state mass balances. In particular, we will derive a shortcut method for evaluation and design of the process shown in Fig. 1. In the first part of this work, we will introduce a formal approach for mass balancing of networks of separation units. Based on this, separation networks can be investigated more easily. In the second part, we will apply the approach to the hybrid separation by SMB chromatography and crystallisation to derive a shortcut evaluation method for this process. The obtained simple algebraic expressions offer valuable insights in the process. In the final part, we will demonstrate the potential of the hybrid process applying the shortcut method and using experimental data from a model system.

2. Balancing approach for networks of binary separation units

The a priori mass balancing and the design of a network of unit operations are usually difficult because the fluxes of the components depend on the (yet unknown) operation conditions in every unit as well as on possible recycles.

Here, we present a formal approach for balancing networks of units capable to separate mixtures of two components (binary separations). At first, we demonstrate the application of the method for the case of a single unit, introducing the conventions used in this work. Then, the approach is extended to networks of binary separation units with and without internal recycles.

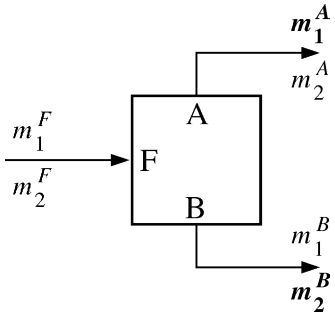

Fig. 2. Single unit for the separation of two compounds (binary fractionator). The target components (bold) are focussed to outlets A (compound 1) and B (compound 2), respectively.

2.1. Single unit

Fig. 2 shows a single unit for the separation of two components (binary fractionator). Such a unit consists basically of a feed node (F) and two outlet nodes (A, B). Throughout this work, we define the outlet compositions as mass or molar fractions with respect to their target components—compound 1 at outlet A and compound 2 at outlet B, respectively (see also the conventions used for process in Fig. 1). The composition of the feed is (arbitrarily) defined with respect to component 1

$$x^{\mathrm{A}} = \frac{m_1^{\mathrm{A}}}{m_1^{\mathrm{A}} + m_2^{\mathrm{A}}} \tag{1a}$$

$$x^{\mathrm{B}} = \frac{m_2^{\mathrm{B}}}{m_1^{\mathrm{B}} + m_2^{\mathrm{B}}} \tag{1b}$$

$$x^{\mathrm{F}} = \frac{m_1^{\mathrm{F}}}{m_1^{\mathrm{F}} + m_2^{\mathrm{F}}} \tag{1c}$$

The x^j are mass or molar fractions, while m_i^j denotes the mass or molar fluxes of component i at the node j. Obviously, for a "successful" separation holds $x^{\mathrm{A}} > x^{\mathrm{F}}$ and $x^{\mathrm{B}} > (1 - x^{\mathrm{F}})$.

The fluxes of the target components leaving the unit, m_1^{A} and m_2^{B}, depend on the inlet fluxes m_i^{F} and the fractions x^{A}, x^{B} and x^{F}. However, we can define the following relative mass fluxes for the target compounds:

$$\frac{m_1^{\mathrm{A}}}{m_1^{\mathrm{F}}} = y_1(x^{\mathrm{A}}, x^{\mathrm{B}}, x^{\mathrm{F}}) \tag{2a}$$

and

$$\frac{m_2^{\mathrm{B}}}{m_2^{\mathrm{F}}} = y_2(x^{\mathrm{A}}, x^{\mathrm{B}}, x^{\mathrm{F}}) \tag{2b}$$

The definitions (2) were also used by Rony [16] who referred to y_i as segregation factors. In the case of a binary separator, y_1 and y_2 correspond to the yields for the two components. It is straightforward to show that from mass balances around the unit in Fig. 2 follows

$$y_1 = \frac{x^{\mathrm{A}}}{x^{\mathrm{F}}} \frac{x^{\mathrm{F}} + x^{\mathrm{B}} - 1}{x^{\mathrm{A}} + x^{\mathrm{B}} - 1} \tag{3}$$

$$y_2 = \frac{x^{\mathrm{B}}}{1 - x^{\mathrm{F}}} \frac{x^{\mathrm{A}} - x^{\mathrm{F}}}{x^{\mathrm{A}} + x^{\mathrm{B}} - 1} \tag{4}$$

The relative fluxes of the target components now follow from Eqs. (1) to (4). For the fluxes of the non-target compounds (component 2 at outlet A and component 1 at outlet B, respectively) holds

$$\frac{m_1^{\mathrm{B}}}{m_1^{\mathrm{F}}} = 1 - y_1 \quad \text{and} \quad \frac{m_2^{\mathrm{A}}}{m_2^{\mathrm{F}}} = 1 - y_2 \tag{5a and b}$$

It is important to note that from Eqs. (2) to (5a and b), the relative mass fluxes or segregation factors are given as functions of the compositions at the nodes of the unit only. Similar approaches are well known in chemical engineering problems. For example, Doherty and Malone [17] used a comparable method for the modelling of flash cascades.

2.2. Interconnected units with and without recycle

Now, we will investigate the balancing of hybrid separation systems, i.e. units integrated on the flowsheet level. Fig. 3 shows two simple networks of binary fractionators that are connected via the outlets of unit I.

Applying the approach above, one can establish relations for all relative fluxes $m_i^{jk}/m_i^{\mathrm{FI}}$ as a function of the y_i^k given by Eqs. (3) and (4). Here, j denotes the node (j = F, A, B) of unit k (k = I, II, ...). The balancing of the system in Fig. 3 (left) is straightforward. As an example, we will look at the relative outlet flux of component 1 at outlet AII in Fig. 3 (left). If there is no recycle, the following expression holds for m_1^{AII}:

$$\frac{m_1^{\mathrm{AII}}}{m_1^{\mathrm{F0}}} = \frac{m_1^{\mathrm{AII}}}{m_1^{\mathrm{FI}}} = y_1^{\mathrm{I}} y_1^{\mathrm{II}} \tag{6}$$

while in the case where a recycle is present

$$\frac{m_1^{\mathrm{AII}}}{m_1^{\mathrm{F0}}} = \frac{y_1^{\mathrm{I}} y_1^{\mathrm{II}}}{1 - \nu y_1^{\mathrm{I}}(1 - y_1^{\mathrm{II}})} \tag{7}$$

Here, ν represents the recycle ratio, i.e. the ratio of mass recycled and m_i^{BII}.

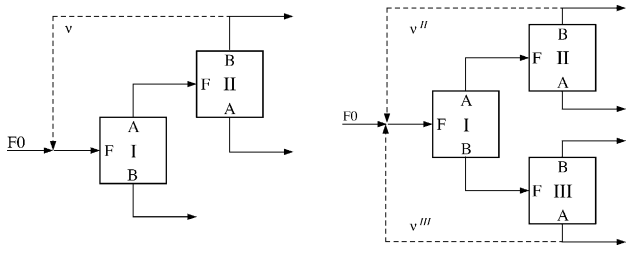

Fig. 3. Examples for interconnected binary fractionators. Left, two units; right, three units. F0 represents the external or total feed to the system. Dashed lines mark optional recycles.

Table 1
Relative mass fluxes for the two components at all positions of the network in Fig. 3 (right)

Unit	Component 1	Component 2
I	$m_1^{\mathrm{AI}}/m_1^{\mathrm{AI}} = y_1^{\mathrm{I}}$	$m_2^{\mathrm{AI}}/m_2^{\mathrm{FI}} = 1 - y_2^{\mathrm{I}}$
	$m_1^{\mathrm{BI}}/m_1^{\mathrm{FI}} = 1 - y_1^{\mathrm{I}}$	$m_2^{\mathrm{BI}}/m_2^{\mathrm{FI}} = y_2^{\mathrm{I}}$
II	$m_1^{\mathrm{AII}}/m_1^{\mathrm{FI}} = y_1^{\mathrm{I}} y_1^{\mathrm{II}}$	$m_2^{\mathrm{AII}}/m_2^{\mathrm{FI}} = (1 - y_2^{\mathrm{I}})(1 - y_2^{\mathrm{II}})$
	$m_1^{\mathrm{BII}}/m_1^{\mathrm{FI}} = y_1^{\mathrm{I}}(1 - y_1^{\mathrm{II}})$	$m_2^{\mathrm{BII}}/m_2^{\mathrm{FI}} = (1 - y_2^{\mathrm{I}}) y_2^{\mathrm{II}}$
III	$m_1^{\mathrm{AIII}}/m_1^{\mathrm{FI}} = (1 - y_1^{\mathrm{I}}) y_1^{\mathrm{III}}$	$m_2^{\mathrm{AIII}}/m_2^{\mathrm{FI}} = y_2^{\mathrm{I}}(1 - y_2^{\mathrm{III}})$
	$m_1^{\mathrm{BIII}}/m_1^{\mathrm{FI}} = (1 - y_1^{\mathrm{I}})(1 - y_1^{\mathrm{III}})$	$m_2^{\mathrm{BIII}}/m_2^{\mathrm{FI}} = y_2^{\mathrm{I}} y_2^{\mathrm{III}}$
F0/FI	$L_1 = \dfrac{m_1^{\mathrm{FI}}}{m_1^{\mathrm{F0}}} = \dfrac{1}{1 - \nu^{\mathrm{II}} y_1^{\mathrm{I}}(1 - y_1^{\mathrm{II}}) - \nu^{\mathrm{III}} y_1^{\mathrm{III}}(1 - y_1^{\mathrm{I}})}$	
	$L_2 = \dfrac{m_2^{\mathrm{FI}}}{m_2^{\mathrm{F0}}} = \dfrac{1}{1 - \nu^{\mathrm{II}} y_2^{\mathrm{II}}(1 - y_2^{\mathrm{I}}) - \nu^{\mathrm{III}} y_2^{\mathrm{I}}(1 - y_2^{\mathrm{III}})}$	

Last row: external (total) and internal (SMB) feed of the process. Feed composition of unit *I* given by Eq. (10).

Similarily, for the system with three units (Fig. 3, right) we obtain without any recycle stream:

$$\frac{m_1^{\mathrm{AII}}}{m_1^{\mathrm{F0}}} = \frac{m_1^{\mathrm{AII}}}{m_1^{\mathrm{FI}}} = y_1^{\mathrm{I}} y_1^{\mathrm{II}} \tag{8}$$

while in the case where the two recycles are present holds

$$\frac{m_1^{\mathrm{AII}}}{m_1^{\mathrm{F0}}} = \frac{y_1^{\mathrm{I}} y_1^{\mathrm{II}}}{1 - \nu^{\mathrm{II}} y_1^{\mathrm{I}}(1 - y_1^{\mathrm{II}}) - \nu^{\mathrm{III}} y_1^{\mathrm{III}}(1 - y_1^{\mathrm{I}})} \tag{9}$$

In order to calculate the segregation factors of unit I, y_i^{I}, the feed composition of this unit, x^{FI}, has to be known. This composition depends on the recycle streams. From a mass balance around the feed node follows

$$x^{\mathrm{FI}} = \frac{\begin{aligned} &K^{\mathrm{I}} K^{\mathrm{II}} K^{\mathrm{III}} x^{\mathrm{F0}} \\ &\quad + \nu^{\mathrm{II}} K^{\mathrm{III}}(1 - x^{\mathrm{BI}})(x^{\mathrm{AI}} - x^{\mathrm{AII}})(1 - x^{\mathrm{BII}} - x^{\mathrm{F0}}) \\ &\quad + \nu^{\mathrm{III}} K^{\mathrm{II}} x^{\mathrm{AI}}(x^{\mathrm{AIII}} - x^{\mathrm{F0}})(x^{\mathrm{BIII}} - x^{\mathrm{BI}}) \end{aligned}}{\begin{aligned} &K^{\mathrm{I}} K^{\mathrm{II}} K^{\mathrm{III}} \\ &\quad + \nu^{\mathrm{II}} K^{\mathrm{III}}(x^{\mathrm{AI}} - x^{\mathrm{AII}})(1 - x^{\mathrm{F0}} - x^{\mathrm{BII}}) \\ &\quad + \nu^{\mathrm{III}} K^{\mathrm{II}}(x^{\mathrm{AIII}} - x^{\mathrm{F0}})(x^{\mathrm{BIII}} - x^{\mathrm{BI}}) \end{aligned}},$$

$$K^k = 1 - x^{\mathrm{A}k} - x^{\mathrm{B}k}, \quad k = \mathrm{I}, \mathrm{II}, \mathrm{III} \tag{10}$$

Expanding this equation leads to a rather voluminous expression. However, in the concrete examples studied below, some assumptions will lead to simple expressions.

In Table 1, all relative mass fluxes of the process scheme in Fig. 3 (right) are listed. To calculate the actual values, the compositions x^{jk} at all nodes of the system, as well as the proper transition conditions have to be specified. The latter are the equality conditions for mass fluxes between units. For example, ($m_i^{\mathrm{FII}} = m_i^{\mathrm{AI}}$, $x^{\mathrm{FII}} = x^{\mathrm{AI}}$) and ($m_i^{\mathrm{FIII}} = m_i^{\mathrm{BI}}$, $x^{\mathrm{FII}} = 1 - x^{\mathrm{BI}}$).[2] The clearly and symmetrically structured equations reveal that mass fluxes at specific points in a network are just the products of the segregation factors of the units passed in the corresponding pathway. This makes the application of the mass balance approach straightforward.

The last line of the table contains the load ratio, L_i, i.e. the ratio between the internal (SMB) feed and the external (total) feed. It represents an important quantity because it is a measure for the additional demand on the SMB process that is caused by recycles. This will be discussed in more detail below.

It should be noted that the process in Fig. 3 (right) represents a superstructure with respect to the process in Fig. 3 (left). The equations in Table 1 are valid also for all possible subsets of the three-unit system. In cases where one of the units or recycle streams is not present in an actual scheme, simply the values for the corresponding y_i^k and ν^k are set to zero.

Above we introduced relative mass fluxes (segregation factors, [16]) for each component, i.e. ratios of the outlet to the feed fluxes. On this basis, it is possible to derive simple mass balance expressions for single units and interconnected binary fractionators with and without internal recycles. The extension of this approach to more complex networks as well as to multicomponent separations appears to be straightforward.

3. Evaluation method for the hybrid separation process

In this section, we will develop a shortcut method for evaluation and design of the hybrid separation process shown in Fig. 1. Although we use here the specific example of combining SMB chromatography and enantioselective crystallisation, it should be noted that the methodology described below is applicable to other process combinations, e.g. membrane separations coupled to chromatography or crystallisation.

There are several design possibilities for the process in Fig. 1. Depending on whether only one of the enantiomers represents the product, or both of them are desired, one of the crystallisers and the corresponding recycle stream will be omitted. As an example, we will investigate the case where the raffinate of the SMB (outlet AI in Fig. 1) contains the desired product. However, the results will be summarised below for the other cases as well, i.e. when the raffinate, or both outlets contain target products.

3.1. Derivation of essential process parameters

Based on the mass balance approach described in the previous section, equations for important process parameters can be derived. In particular these are overall *yield*, *recycle ratio*, and internal *load* of the SMB process.

3.2. Mass fluxes, yield, and recycle ratio

All necessary expressions for the mass fluxes are listed in Table 1. A few conventions are necessary to apply the

[2] Feed compositions are defined with respect to component 1, thus $x^{\mathrm{FII}} = 1 - x^{\mathrm{BI}}$, see Eq. (1c).

equations. According to Fig. 1, the raffinate AI is enriched in enantiomer 1, while the extract BI contains an excess of enantiomer 2. Because in our example the raffinate contains the product of interest, the target product is withdrawn at outlet AII. The crystalliser III and its recycle are omitted ($y^{III} = 0$, $\nu^{III} = 0$). To allow for crystallisation of pure enantiomer ($x^{AII} = 1$), the purity of the raffinate always has to exceed a specific eutectic composition x^E [15], i.e. $x^{AI} > x^E$.[3] From these conventions and Eqs. (3) and (4) follows for the segregation factors of the target component (index "1" omitted):

$$y^I = \frac{x^{AI}}{x^{FI}} \frac{x^{FI} + x^{BI} - 1}{x^{AI} + x^{BI} - 1} \tag{11}$$

$$y^{II} = \frac{x^{AI} + x^{BII} - 1}{x^{AI} x^{BII}} \tag{12}$$

These two equations can be substituted into Eq. (7) to generate an expression for both the relative mass flux of the target component as well as the overall yield of the process, Y:

$$Y = \frac{m_1^{AII}}{m_1^{F0}} = \frac{y_1^I y_1^{II}}{1 - \nu^{II} y_1^I (1 - y_1^{II})} \tag{13}$$

If the process should achieve a certain overall yield Y^*, Eq. (13) can be rearranged to obtain the necessary recycle ratio:

$$\nu^{II} = \frac{Y^* - y^I y^{II}}{Y^* y^I (1 - y^{II})} \tag{14}$$

To calculate values for y^I and y^{II}, the feed purity x^{FI} can be calculated from Eq. (10). However, as mentioned earlier, this expression can be simplified significantly. Because enantiomers usually represent expensive products, high yields appear desirable. The latter can be achieved by high recylce ratios. Assuming complete recycle, i.e. $\nu^{II} = 1$, and a racemic total feed ($x^{F0} = 0.5$), Eq. (10) reduces to

$$x^{FI}(\nu = 1) = \frac{\begin{array}{c} 2x^{AI}x^{BI}x^{BII} + x^{AI} + x^{BI} + x^{BII} \\ - x^{AI}x^{BI} - x^{BII}(x^{AI} + x^{BI}) - 1 \end{array}}{2x^{BII}x^{BI} + x^{AI} - 1} \tag{15}$$

A further increase of the yield results from demanding that the extract (BI) should contain only the non-target enantiomer 2, i.e. $x^{BI} = 1$. Then, it follows from (15)

$$x^{FI}(\nu = 1, x^{BI} = 1) = \frac{x^{AI}x^{BII}}{2x^{BII} + x^{AI} - 1} \tag{16}$$

It should be noted that in this case $y^I = 1$.

The assumption of pure extract at first might appear somewhat contradictory, because the economical advantage expected from the hybrid process is based on reducing purity requirements on SMB. However, because any of the target enantiomer leaving the process via the outlet of the non-target species (in this example, the extract) is lost, in order to limit costs it might often be mandatory to maintain the latter outlet pure. In this case, the possible benefit will result only from the lowered purity requirements on the outlet of the target enantiomer (in this example, the raffinate).

3.3. Internal load on SMB process

An important issue about the configuration in Fig. 1 is that the yield of the crystalliser is restricted by the position of the eutectic. The higher the eutectic purity, the less crystals are produced, and more material has to be recycled back to the feed node to maintain the overall yield. This recycling process causes additional load on the SMB, and thus, decreases overall throughput.

As mentioned above, this fact is quantified by the ratio between SMB feed and total feed, $L_i = m_i^{FI}/m_i^{F0}$ (see Table 1). For the case when enantiomer 1 (raffinate) constitutes the target product, we obtain for the load L_1 from Table 1 and the conventions above

$$L_1 = \frac{m_1^{FI}}{m_1^{F0}} = \frac{1}{1 - \nu^{II} y^I (1 - y^{II})} \tag{17}$$

For a stand-alone separation by SMB, there is no recycle and thus $L_1 = 1$, i.e. $m_1^{FI} = m_1^{F0}$. As soon as a recycle is present, the SMB has to process a mass flux higher than the external feed, i.e. $L_1 = 1$ or $m_1^{FI} > m_1^{F0}$.

The possible throughput of the hybrid process is determined by (i) the benefit arising from lowered purity requirements on SMB and (ii) the position of the eutectic. Only if the managable throughput rises strongly enough with lower SMB outlet purity, it will counterbalance the additional load imposed by the recycle. Fig. 4 demonstrates this interrelation for a generic, but typical function, see e.g. [9]. If the dependence of the SMB throughput on purity, $m_i^{FI}(x^I)$, is known, the external feed of the process, m_i^{F0}, follows from Eq. (17).

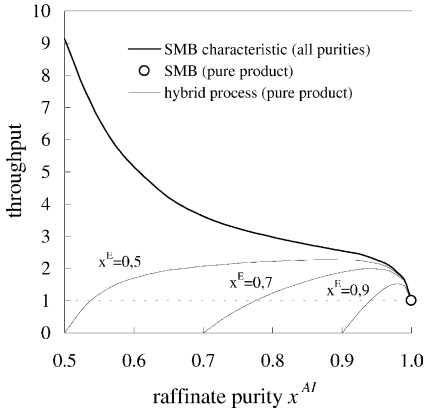

Fig. 4. Typical dependency of SMB throughput on purity requirements (generic example of a purity-performance characteristic, thick line). From this characteristic, the possible throughput of a hybrid process (thin lines) is calculated as a function of the eutectic composition (complete recycle, Eq. (17)). Obviously, the hybrid process can be more productive than a stand-alone separation by SMB (symbol).

[3] In this work, the eutectic purity is defined with respect to component 1. For conglomerate forming systems, $x^E = 0.5$. For compound forming systems, $0.5 < x^E < 1$. (For details, see [15].)

Table 2
Main process parameters and conventions for the three process options

Target(s)	Raffinate[a]	Extract[a]	Raffinate and extract
Units	I, II	I, III	I, II, III
Conventions	$x^{AI} > x^{E}$	$x^{BI} > x^{E}$	$(x^{AI} = x^{BI}) > x^{B}$
	$x^{AII} > 1$	$x^{BIII} > 1$	$x^{AII} = x^{BIII} = 1$
	$x^{FII} = x^{AI}$	$x^{FIII} > 1 - x^{BI}$	$x^{FII} = x^{AI}$, $x^{FIII} = 1 - x^{BI}$
Segregation factors	$y^{I} = \frac{x^{AI}}{x^{FI}} \frac{x^{FI} + x^{BI} - 1}{x^{AI} + x^{BI} - 1}$	$y^{I} = \frac{x^{BI}}{1 - x^{FI}} \frac{x^{AI} - x^{FI}}{x^{AI} + x^{BI} - 1}$	$y^{I} = x^{I}$
	$y^{II} = \frac{x^{AI} + x^{BII} - 1}{x^{AI} x^{BII}}$	$y^{III} = \frac{x^{AIII} + x^{BI} - 1}{x^{AIII} x^{BI}}$	$y^{II} = \frac{x^{I} + x^{II} - 1}{x^{I} x^{II}}$
Feed composition	$x^{FI} = \frac{x^{AI} x^{BII}}{2x^{BII} + x^{AI} - 1}$[b]	$x^{FI} = \frac{x^{AIII}(2 - x^{BI}) + x^{BI} - 1}{2x^{AIII} + x^{BI} - 1}$[b]	$x^{FI} = x^{F0}$
SMB load	$L = \frac{1}{1 - \nu^{II} y^{I} (1 - y^{II})}$	$L = \frac{1}{1 - \nu^{III} y^{I} (1 - y^{III})}$	$L = \frac{1}{1 - \nu(1 - y^{I} y^{II})}$
Yield[a]	$Y = \frac{y^{I} y^{II}}{1 - \nu^{II} y^{I} (1 - y^{II})}$	$Y = \frac{y^{I} y^{III}}{1 - \nu^{III} y^{I} (1 - y^{III})}$	$Y = \frac{x^{I} + x^{II} - 1}{x^{II} - \nu(1 - x^{I})}$
Recycle ratio	$\nu^{II} = \frac{Y - y^{I} y^{II}}{Y y^{I} (1 - y^{II})}$	$\nu^{III} = \frac{Y - y^{I} y^{III}}{Y y^{I} (1 - y^{III})}$	$\nu = \frac{x^{II} Y - (x^{I} + x^{II} - 1)}{Y(1 - x^{I})}$

[a] Segregation factors, yields, and loads defined with respect to target component.
[b] For $x^{F0} = 0.5$, complete recycle ($\nu = 1$), and pure non-target component from SMB (see text).

The external feed increases for decreasing recycle ratio, decreasing eutectic composition, and increasing SMB purity.

3.4. Summary of process parameters

Table 2 lists the process parameters derived for the three different cases. If both enantiomers are of interest, we use a "symmetrical" operation scheme, i.e. we assume identical operating conditions ($x^{AI} = x^{BI} = x^{I}$, $x^{BII} = x^{AIII} = x^{II}$, $\nu^{II} = x^{III} = \nu$) in the two branches of the process in Fig. 1.

3.5. Concept of a shortcut method

The key of the approach suggested is to reduce the evaluation problem to the determination of purity-performance characteristics like the one shown in Fig. 4. Here we assume that (i) the SMB process is the limiting step in the system, and (ii) that this justifies the description of the crystallisation as an equilibrium operation.[4] These assumptions allow to use the mass balance approach above for calculation of mass fluxes and essential process parameters from the purity-performance characteristics. Based on this, we suggest the following procedure for process evaluation:

(1) *Determination of required parameters* from measurements and/or correlations.
(2) *Specification of process requirements* (e.g. the overall yield required). From this, restrictions follow on necessary outlet purities and recycle ratio.
(3) *Determination of purity-performance characteristics* of the SMB (see Fig. 4). This follows from optimisations of a suitable model. A proper objective function has to be used.
(4) *Determination of essential process parameters of the hybrid process.* Essential parameters are the load ratio L, the total throughput m_i^{F0} (see Table 2), and the necessary volume of CSP.

It should be noted, that steps (2)–(4) could well be performed in a single step by including all relations into a model for the whole process. However, the advantage of decomposing the problem into the steps listed above is that the optimisation results can be re-used if certain conditions (e.g. column geometry or pressure drop restriction) change.

4. Evaluation of a concrete example

In this chapter, we will investigate the separation of the enantiomers of mandelic acid. Three process alternatives resulting from the choice of the target enantiomer(s) are studied. In cases I and II, the extract and the raffinate deliver the target enantiomer, respectively. In case III, both enantiomers are desired.

4.1. Procedure

The procedure used for the evaluations corresponds to the concept explained above. The following steps were realised:

(1) *Determination of required parameters*. The parameters necessary to perform this analysis are: adsorption isotherms, position of the eutectic, and relations for pressure drop and plate number as functions of the flow rate. Section 4.2 summarises experimental procedures and results.

[4] Assumption (ii) can be satisfied by guaranteeing that the residence time in the crystalliser is high enough to achieve thermodynamic equilibrium. This can be achieved, e.g. by using large or a series connection of crystallisers.

(2) *Specification of process requirements.* For all cases studied here, we assume a minimum overall yield for the target enantiomer of $Y = 0.998$. To achieve this value, in all three cases high recycle ratios are necessary. For sake of simplicity, we assume complete recycle ($\nu = 1$) for cases I and II. From this, it follows from the relations for the yield in Table 2, that in case I, $x^{AI} = 0.998$, and in case II, $x^{BI} = 0.998$.

(3) *Determination of purity-performance characteristics* from a model. Here, we use a simple steady state model for the true moving bed (TMB) process. TMB models are numerically less expensive than SMB models; in particular if only the steady state is of interest. Thus, their fast performance allows for systematic parameter studies. For fundamentals of modeling TMBs see e.g. [18,19]. The TMB model used here is summarised in Appendix A.1.

Optimisations were performed for plate numbers between 2 and 100 (per zone), and different outlet purities $x^E = 0.7 < x^I < 0.998$ (x^I denotes the SMB outlet containing the target enantiomer). To maximise throughput, the feed concentration should be as high as possible [9,10,20]. Thus, the highest concentration used in the isotherm measurements was taken, i.e. $c_i^{F0} = 7.5$ g/l (see below). The feed composition x^{FI} is calculated from Table 2.

At early stages of process development it is sufficient to use a "reasonable" objective function. It is desirable to maximise throughput and to minimise eluent consumption [21]. Thus, we use the ratio between throughput and solvent requirement as objective. For the three cases, the objective functions are: $OF = Q^D/(Q^{BI}c_2^{BI})$ (case I), $OF = Q^D/(Q^{AI}c_1^{AI})$ (case II), and $OF = Q^D/(Q^{AI}c_1^{AI} + Q^{BI}c_2^{BI})$ (case III). Here, Q^D, Q^{AI}, and Q^{BI} denote volumetric flow rates of desorbent, raffinate and extract, respectively. The c_i^j denote concentrations.

(4) *Determination of essential process parameters*. Because a TMB model is used here, at first the bed lengths (or CSP volume) and possible flow rates that correspond to the use of packed columns (as used in SMB processes) are calculated using correlations for pressure drop and plate number as a function of flow rate. This is explained in Appendix A.2. For each optimisation performed, the load ratio, L, and the overall throughput, m_i^{F0}, can be calculated from Table 2. Any further information available can be included in the evaluation procedure. For example, from the solubility of the eutectic composition (see 4.2), the amount of solvent can be calculated that has to be removed between SMB and crystallisation. More details can be found in Appendix A.3.

4.2. Experimental parameter estimation

4.2.1. Chromatographic system

For the chromatographic separation of the mandelic enantiomers we used Chirobiotic T (ASTEC, UK) as the stationary phase, packed into a stainless column (150 mm × 10 mm) (Muder&Wochele, Germany). The mobile phase was 80/20 (v/v) 0.3 M triethyl ammonium acetate buffer/methanol. This eluent was shown by others to be applicable for the system [22]. It was prepared mixing 1 M triethyl ammonium acetate (Calbiochem, U.S.A.) with deionised water (further purified with a Milli-Q-Gradient system, Millipore, U.S.A.) to prepare a 0.3 M solution. The pH-value of the buffer solution was adjusted to 4.1 using acetic acid (>99.8%, Merck, Germany). The buffer then was mixed with gradient grade methanol (Merck, Germany). The HPLC-system was an HP1100-system (Agilent, U.S.A.), consisting of a quaternary low-pressure gradient pump, an autosampler, and a DAD. The detection was performed at 254 nm in the low concentration range and at 275 nm for large concentrations. The flow rate was verified permanently using a flow meter (Phase Separations, U.K.).

4.2.2. Porosity and adsorption isotherms

The total porosity, ε_t, was determined as $\varepsilon_t = 0.775$ from injections of mobile phase. The initial slopes of the mandelic acid isotherms on the Chirobiotic T (Astec, UK) stationary phase were determined by 10 μl injections of 2.5 g/l mandelic acid (>99%, Merck, Germany) solutions. Determination of the isotherms was done using a perturbation method [23–25]. The experiments were performed at a flow rate of 2.5 ml/min. The low-pressure gradient pump was used to provide the concentration plateaus (10 steps up to $c_{rac} = 15$ g/l). At concentrations higher than 15 g/l, no separation was achieved. On each plateau, 20 μl injections of mobile phase were performed. Table 3 shows the measured retention times of the two peaks resulting from each injection.

The retention times were fitted to an isotherm model using a least-square method. The bi-Langmuir isotherm equation with one unselective and one selective site as suggested by Jandera et al. [22] fitted well the perturbation results:

$$q_i = q^I \frac{b_i^I c_i}{1 + \sum_j b_j^I c_j} + q^{II} \frac{b_i^{II} c_i}{1 + \sum_j b_j^{II} c_j} \quad (18)$$

4.2.3. Pressure drop and column efficiency

Dependence of pressure drop and theoretical plate height on flow rate were determined experimentally in the range of

Table 3
Retention times measured in perturbation experiments

c_{rac} (g/l)	$t_{R,1}$ (min)	$t_{R,2}$ (min)
0	4.80	7.07
0.375	4.73	6.22
0.75	4.69	5.94
1.5	4.67	5.70
2.25	4.65	5.52
3	4.62	5.37
4.5	4.59	5.17
6	4.56	5.07
9	4.52	4.91
15	4.47	4.76

Table 4
Parameters determined experimentally

q^{I} (g/l)	142
$b_1^{I} = b_2^{I}$ (l/g)	0.0073
q^{II} (g/l)	3.19
b_1^{II}(l/g)	0.0273
b_2^{II} (l/g)	0.7041
ε_t (–)	0.775
A (min)	0.0017
B (cm)	0.0082
k_0 (bar min/cm^2)	0.2232
x^{E} (–)	0.7
S^{E} (5 °C) (g/l)	215

0.5–10.0 ml/min. From analytical injections, a mean value of the plate heights of the two enantiomers was taken. In the range covered a linear dependency was found. Thus, a linearised van-Deemter equation is applied here:

$$\mathrm{HETP} = Au_0 + B \tag{19}$$

In this equation, $u_0 = 4Q/(\pi D^2)$ is the superficial velocity; Q, the flow rate; and D, the column diameter.

For the Chirobiotic T column used, the pressure drop depends linearly on the superficial velocity:

$$\frac{\Delta p}{L_C} = k_0 u_0 \tag{20}$$

In this Darcy-like equation, L_C is the column length and k_0 a proportionality parameter.

4.2.4. Solubility

The eutectic composition of the mandelic acid system is approximately $x^{E} = 0.7$ [26]. The solubility of this composition in the mobile phase, S^{E}, was measured at a temperature of $T = 5\,^{\circ}\mathrm{C}$ [27]. This was done by equilibrating (stirring) the solvent with a surplus of solid for 24 h and subsequently analysing the liquid by HPLC. The temperature was controlled to ±0.1 K (Polystat CC3 thermostat, Huber Kältemaschinenbau, Germany). The value determined is 215 g/l.

The parameters determined experimentally (porosity, adsorption isotherms, pressure drop, and plate height, solubility) are summarised in Table 4.

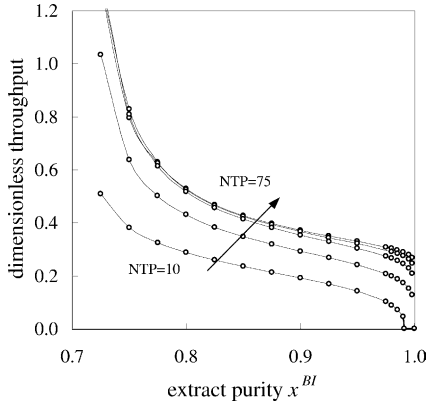

Fig. 5. Purity-performance characteristics (dimensionless product fluxes) of a TMB for different number of stages (case II, extract is desired product). Results for plate number NTP = 10, 15, 30, 50, 75 per zone (from bottom up).

4.3. Results of evaluation procedure

4.3.1. Case I: target product from extract

Fig. 5 shows the results of the TMB optimisations (see Appendix A) for the case when the extract delivers the desired enantiomer 2. For different plate numbers, the dimensionless productivity of the TMB as a function of the extract purity is shown. This dimensionless product flux, $(\gamma^{(1)} - \gamma^{(2)})c_2^{BI}/c_2^{F0}$, is directly proportional to the mass flux of target enantiomer, m_2^{BI}. Due to the thermodynamic properties of the system, the possible productivity rises significantly with lowering purity requirements. For example, if each zone has a plate number of NTP = 75, the productivity can be doubled if purity requirement is lowered from

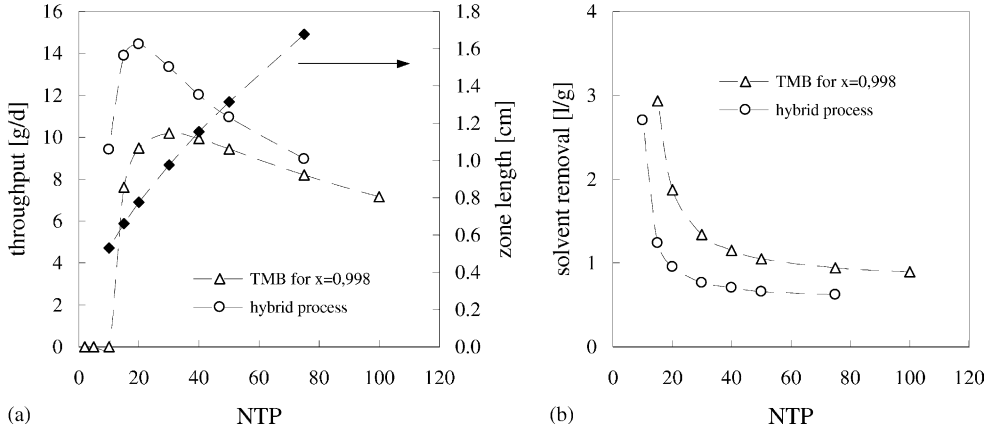

Fig. 6. (a and b) Performance of stand-alone separation by SMB and hybrid process for case I (extract contains target enantiomer). Flow rates, bed lengths (CSP volumes), and relative solvent removal as a funtion of number of stages/zone of the TMB. The hybrid process outperforms the stand-alone separation by SMB.

$x^{BI} = 0.998$ to 0.8. This typical behaviour was demonstrated before for SMB processes [9,10,28]. If the plate number is very low (for example, NTP = 10 in Fig. 5), pure product cannot be achieved. However, for low purity requirements still considerable throughputs are possible.

Fig. 6a shows the throughput flow rates and the necessary bed length calculated from all TMB optimisations performed (see Appendix A.2). For the separation by SMB alone, the calculations predict a throughput-optimum at 30 theoretical stages per zone (desired purity is $x^{BI} = 0.998$). However, the hybrid process (that delivers pure product, i.e. $x^{BIII} = 1$) clearly outperforms this. At 20 stages/zone, the throughput is 43.6% higher than in the stand-alone separation. Simultaneously, the zone length (and thus the volume of CSP) is 20.5% lower. Fig. 6b shows the relative amount of solvent that has to be removed (for calculation procedure, see Appendix A.3). In the stand-alone separation, the solvent has to be removed completely to obtain a solid powder. For the throughput-optimum (NTP = 30), about 1.33 l of solvent per gram target product are evaporated. In the hybrid process, at NTP = 20 only 0.95 l/g (−28.7%) have to be removed to reach the concentrations level necessary to crystallise at $T = 5\,^{\circ}C$.

4.3.2. Case II: target product from raffinate

In analogy to Fig. 6, Fig. 7a and b show the performances for the stand-alone separation by SMB ($x^{AI} = 0.998$) and for the hybrid process ($x^{AII} = 1$). Obviously, throughput, CSP volume, and relative solvent removal of the two options are similar; the hybrid process appears only slightly better than the stand-alone SMB, i.e. throughput and solvent removal improve by 10%, while the same amount of chiral stationary phase is necessary. Because of the additional efforts necessary for design and implementation of a hybrid process, this case is not regarded as being advantageous. Probably, it would be more straightforward to design and use the SMB in stand-alone mode for a separation.

The reason for the comparably low improvements is the behaviour of the concentration waves inside of the SMB (or TMB) unit. For decreasing purity requirements, the internal shock waves become higher and, thus, are travelling faster within the separation zones [29]. At the same, high extract purity has to be maintained to meet the yield requirements (see above). With decreasing raffinate purity, the optimisations return lower values for $\gamma^{(4)}$ and higher desorbent flow rates to counterbalance these effects. This restricts the overall throughput possible.

4.3.3. Case III: target products from extract and raffinate

In this case, we assumed "symmetrical" operation of the plant, i.e. in each optimisation we required identical raffinate and extract purity. It is noteworthy that the recycle ratio does not have to be one in this case to meet the yield requirement of $Y = 0.998$. Instead it depends on the SMB outlet purity and can be calculated for every optimisation from Table 2.

If both enantiomers are desired products, similar performance improvements as in case I can be achieved (Fig. 8a and b). Comparing the throughput-optima for the stand-alone SMB process (at NTP = 30 stages/zones) and for the hybrid system (NTP = 15 stages/zone), we find that in the hybrid scheme the throughput is 78% higher, while CSP volume is 45.7% lower. The solvent removal is almost identical. However, by giving in some of the throughput, the solvent removal decreases by 13% (NTP = 20) or 24% (NTP = 30), respectively, while the throughput is still significantly higher if compared to the stand-alone process.

4.3.4. Remarks and limitations of the approach

It represents an interesting fact that very low values were found for the optimum number of theoretical plates (NTP). On one hand, this stresses the significant potential to save investment costs for CSP by combining SMB and crystallisation. Alternatively, less efficient (and less expensive) CSPs and solvents could be used to resolve the separation task without increasing operation costs. On the other hand, the low optimal plate numbers indicate that the application of hybrid separation schemes might facilitate using simpler separation processes, because it actually appears rather contradictory to design a complicated process like SMB for a low-efficiency system requiring only 10 theoretical stages. The implemen-

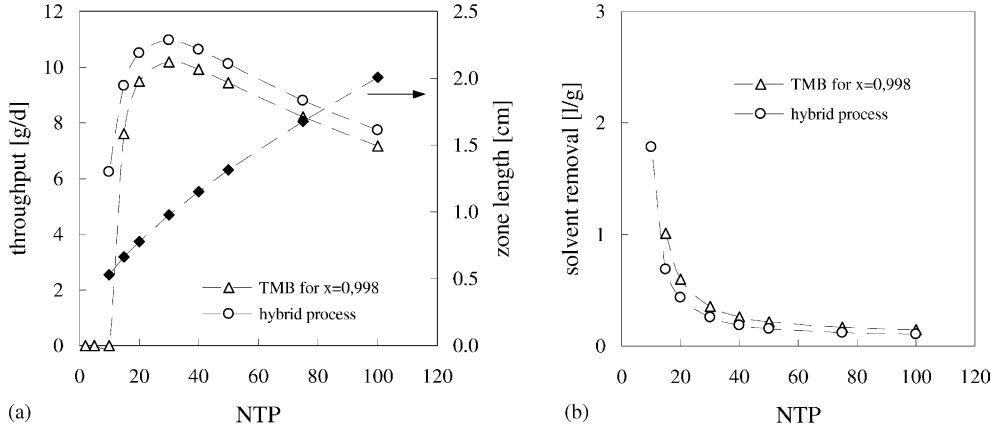

Fig. 7. (a and b) Calculated flow rates, CSP volumes (bed lengths), and solvent removal before crystallisation if the raffinate contains the enantiomer of interest.

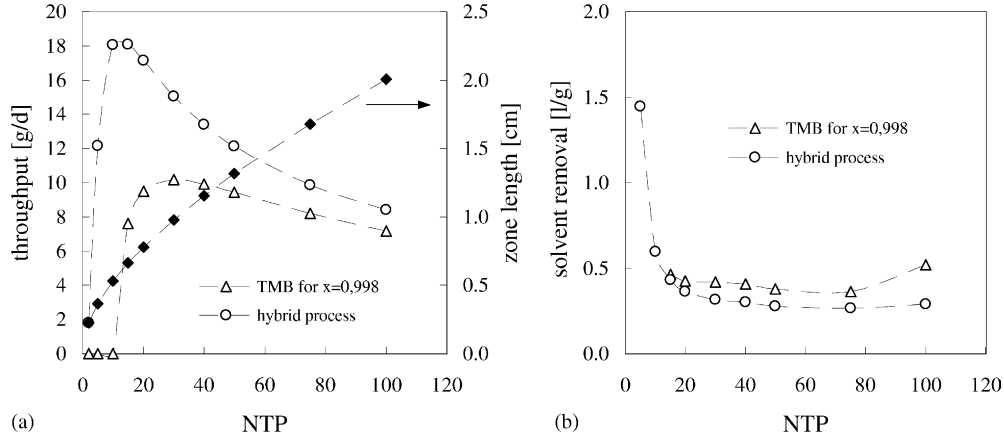

Fig. 8. (a and b) Flow rates, CSP volumes (bed lengths), and solvent removal (average value for both branches) if both enantiomers are desired. For solvent removal, average values for the two enantiomers are used.

tation of less efficient techniques like membrane processes might be of interest.

From the calculations for cases I–III, some limitations of the approach should be mentioned. The values for the performance parameters obtained from the approach above will not match exactly the values that can be used in an SMB. One issue is that the optimal bed lengths obtained are rather low (between 0.5 and 2 cm), while simultaneously high flow rates are applied (up to 50 ml/min). These cannot be used in a real SMB, because it would cause impractically short switching times (in the range of a few seconds). Because of the high pressure drop and efficiency of the column used, these high flow rates could not be covered by the measurements. Another limitation is that a TMB model always overpredicts SMB performance. However, in our experience the purity-performance characteristics of SMB and TMB models are very similar in their shape. For $x^{I} < 0.95$, they are almost identical. The main difference is that the SMB needs a higher plate number to achieve the same performance. It appears a valid strategy to compare some SMB and TMB calculations for a given separation problem to quantify the differences between model predictions. However, this is out of the scope of this work.

We want to stress that—despite the aforementioned limitations—the approach presented will predict the trends of the system correctly, while the actual results will represent the upper limits of the benefits achievable from the hybrid process.

5. Conclusions

In this work, we presented a shortcut approach for a first-stage evaluation of hybrid separation processes. Key of the method is the determination of the purity-performance characteristic of the performance-limiting step in the process scheme. Once this characteristic is known, the whole process scheme can be evaluated based on the rigorous application of mass balances. The use of relative mass fluxes (segregation factors) leads to simple algebraic relations for mass balances and essential process parameters, even in rather complicated networks involving recycles. This general strategy is not limited to the concrete example discussed in this paper but can easily be adopted to other separator networks.

In the evaluation of enantioseparations by coupled SMB chromatography and selective crystallisation, the use of a TMB model facilitates fast predictions of characteristics and allows for systematic parameter studies. Beneficial process configurations can be identified that arise from the choice of the target enantiomer(s). The performance of the scheme is influenced by several factors, most importantly by the position of the eutectic (which determines the per-pass-yield of the crystallisation as well as necessary internal recycles), the shape of the purity-performance characteristic (which is governed by the adsorption equilibrium), and the absolute flow rates and necessary CSP volume (affected mainly by pressure drop and column efficiency).

For the concrete example studied (the separation of mandelic acid enantiomers on Chirobiotic T), we demonstrated that the hybrid process possesses a significant potential to reduce operating costs. In case I (target is the more retained enantiomer) and case III (both enantiomers are targets), the hybrid process clearly outperforms the stand-alone separation by SMB chromatography. As an example, in case I, it is possible to simultaneously increase throughput by 44%, to decrease CSP volume by 20%, and to decrease solvent removal by 29%. In case II (less retained enantiomer is desired), only slight improvement is achieved, while in case III (both enantiomers are desired), the throughput might be increased by 78%.

While for this work, solubilities were measured in the chromatographic solvent, the possibility of a complete solvent exchange should be mentioned. The latter might be necessary, for example, if components of the chromatographic solvent tend to crystallise, if a polymorph depends on the type of solvent, or if the solubility is too high.

Like for every shortcut method, some limitations arise from the simplifications made. Bed lengths and absolute flow rates calculated from TMB optimisations cannot be expected to match exactly the values applicable in a real SMB plant. However, the method correctly predicts the trends of the system and allows the estimation of potential benefits. Because only a minimum of experimental information is necessary, it is applicable for first-stage evaluations. Alternatively, the approach can be used as a starting point for more detailed investigations, e.g. by generation of initial conditions for multi-level optimisations (MLOP), or by definition of limits for stochastic optimisation procedures like genetic algorithms [30].

The results emphasise that in integrated schemes for enantioseparations it might also be of interest to use unit operations that are less efficient and thus probably less expensive than SMB chromatography. This might apply, for example, to membrane-based process.

Acknowledgements

The authors would like to thank Mr. D. Sapoundjiev for the measurement of solubility data. The financial support by Schering AG (Berlin) and by the German Ministry of Research and Education (BMBF) through project NMT/CT/02C0319A is gratefully recognized.

Additional material

To demonstrate our approach, a rather large number of TMB optimisations were performed—more than actually are necessary in practice. For sake of clarity, we did not present the raw data of these TMB optimisations. These data are available from the authors.

Appendix A

A.1. TMB model

The TMB model is a continuous approximation of the SMB process. In this work, the TMB process is modelled as a series-connection of equilibrium stages. The model consists of the mass balances for the components (i) in all stages (k) of the four zones (j) of the TMB:

$$\frac{\partial c_{i,k}}{\partial t} = \frac{1}{\varepsilon V}\{Q_S[q_{i,k+1}(\bar{c}_{k+1}) - q_{i,k}(\bar{c}_k)] + Q_{k-1}^{(j)} c_{i,k-1} - Q_k^{(j)} c_{i,k} \pm Q_{ext} c_{i,ext}\} \quad i = 1, 2, \quad k = 1, \ldots, N, \quad j = 1, \ldots, 4 \quad (A.1)$$

Q_{k-1} and Q_k denote volumetric flow rates for the liquid phase entering and leaving the stage, respectively. Q_{ext} and $c_{i,ext}$ are external fluxes and concentrations for stages with in- or outlet (feed, desorbent, raffinate, extract), for all other stages holds $Q_{ext} = 0$. Q_S is the solid flow rate identical in all stages. The solid phase loading is q_i, which is given by the adsorption isotherm (see Chapter 4). V and ε are volume and porosity of a single stage.

This simple model was implemented in the simulation environment DIVA using the modeling tool PROMOT [31,32]. Because here only steady state results are of interest, the model can be further simplified by setting $\partial c_{i,k}/\partial t = 0$. In this case, it reduces to a set of nonlinear equations that can be solved using standard software packages. It remains an option to extend the study using more detailed models of the continuous SMB process. Ruthven and Ching [19] and, more recently, Guiochon [18] presented comprehensive overviews on possible modeling approaches.

A sequential quadratic programming (SQP) optimisation method available in DIVA [33] was used. SQP was used successfully for SMB optimisations by other authors, e.g. [34]. Optimisation variables are the dimensionless internal flow rates, $\gamma^{(j)}$, for the four zones j of the TMB:

$$\gamma^{(j)} = \frac{Q_{TMB}^{(j)}}{Q_S} \quad (A.2)$$

The $\gamma^{(j)}$ correspond to the m_j in [20]. For more details concerning the use of $\gamma^{(j)}$, see [20] and below.

A.2. Flow rates and bed lengths corresponding to NTP-values in TMB optimisations

The TMB process is not used in practice because of the problems arising from solid handling (backmixing and abrasion). Thus, flow rates and bed lengths that correspond to the use of packed columns (as are used in SMB processes) have to be calculated.

The pressure drop in an SMB depends on the configuration of zones and pumps, for details see [35]. The highest internal flow rates and thus the highest throughputs are guaranteed if the maximum tolerable pressure drop, Δp_{max}, is achieved. For the Chirobiotic T column, Δp is given by (20). In SMB systems with one internal recycle pump, Δp depends on all four internal flows. Assuming identical zone lengths, from (20), we obtain

$$\Delta p_{max} = 4 k_0 L_C \frac{Q_{t,SMB}}{\pi D^2} \quad (A.3)$$

where Q_t is the sum of all four internal flow rates. For the maximum pressure drop tolerable, we assume $\Delta p_{max} = 50$ bar.

The relation between the height of a theoretical plate, HETP, and the flow rate is given by Eq. (19). For a plate number averaged over all four zones, $\overline{NTP}$, it follows from (19)

$$\overline{NTP} = \frac{L_C}{\overline{HETP}} = \frac{L_C}{A\bar{u}_0 + B} = \frac{L_C}{A(Q_{t,SMB}/\pi D^2) + B} \quad (A.4)$$

From (A.3) and (A.4), the flow rates and zone length can be calculated that correspond to the $\overline{\text{NTP}}$ used in the TMB optimisations and to the tolerable pressure drop, $\Delta p_{\max}$ and solving (A.3) and (A.4) for the bed length L_C, we obtain

$$L_C = \frac{1}{2k_0}[\text{NTP}Bk_0 + \sqrt{\text{NTP}k_0(\text{NTP}k_0B^2 + A\Delta p_{\max})}] \tag{A.5}$$

For each TMB optimisation, the sum of the flow rates $Q_{t,SMB}$ and the bed length L_C now are calculated from Eqs. (A.3) and (A.5). Please note, that if the correlations for $\Delta p_{\max}$ and HETP are nonlinear, some simple iteration has to be used.

The zone flow rate in an SMB, $Q_{SMB}^{(j)}$, depends on $\gamma^{(j)}$ [20]:

$$Q_{SMB}^{(j)} = \frac{\gamma^{(j)}V_C(1-\varepsilon_t) + V_C\varepsilon_t}{t_S} \tag{A.6}$$

Here, t_S and $V_C = \pi D^2 L_C$ are the switching time and column volume, respectively. From (A.6) and $Q_{t,SMB} = \sum_j Q_{SMB}^{(j)}$ follows for the flow rate in an individual zone

$$Q_{SMB}^{(j)} = Q_{t,SMB}\frac{\gamma^{(j)}(1-\varepsilon_t) + \varepsilon_t}{(1-\varepsilon_t)\sum_j \gamma^{(j)} + 4\varepsilon_t} \tag{A.7}$$

From (A.7) all individual zone flow rates can be obtained from the $\gamma^{(j)}$ and $Q_{t,SMB}$. The external flow rates (feed, desorbent, raffinate, extract) follow from the corresponding relations, i.e. $Q_{SMB}^{FI} = Q_{SMB}^{(3)} - Q_{SMB}^{(2)}$, $Q_{SMB}^{AI} = Q_{SMB}^{(3)} - Q_{SMB}^{(4)}$, $Q_{SMB}^{BI} = Q_{SMB}^{(1)} - Q_{SMB}^{(2)}$, and $Q_{SMB}^{D} = Q_{SMB}^{(1)} - Q_{SMB}^{(4)}$.

A.3. Calculation of solvent removal

Another important aspect is related to solubility. If concentrations delivered by the SMB are lower than needed for crystallisation, some solvent has to be removed before or within the crystallisation step. The relative solvent removal (litres solvent removed per gram of product) can be calculated from the SMB outlet purity (e.g. x^{AI}) and the overall solubility of the eutectic, $S^E(T)$. One value for $S^E(T)$ has to be known. In the example where the raffinate contains the target, the non-target enantiomer 2 is not crystallised out, thus $c_2^{E*} = c_2^{FII}$. Then, we obtain from $S^E(T) = c_1^{E*} + c_2^{E*}$, $x^E = c_1^E/(c_1^E + c_2^E)$, and $x^{FII} = x^{AI} = c_1^{FII}/(c_1^{FII} + c_2^{FII})$, for the crystallisation inlet concentration of the target:

$$c_1^{FII}(T) = S^E(T)x^{AI}\frac{1-x^E}{1-x^{AI}} \tag{A.8}$$

The relative amount of solvent to be removed now follows from (A.8):

$$\frac{Q^{AI} - Q^{FII}}{m_1^{AII}} = \frac{c_1^{FII}(T) - c_1^{AI}}{c_1^{FII}(T)}\frac{Q^{AI}}{m_1^{AII}} \tag{A.9}$$

Q^{AI} and c_1^{AI} are the flow rate and concentration of the raffinate, respectively (known from the TMB optimisations).

References

[1] H.E. Schoemaker, D. Mink, M.G. Wubbolts, Science 299 (2003) 1694.
[2] T.P. Yoon, E.N. Jacobsen, Science 299 (2003) 1691.
[3] G. Subramanian, A Practical Approach to Chiral Separations by Liquid Chromatography, VCH, Weinheim, 1994.
[4] F. Gasparrini, D. Misiti, C. Villani, J. Chromatogr. A 906 (2001) 35.
[5] E. Yashima, J. Chromatogr. A 906 (2001) 105.
[6] P. Franco, A. Senso, L. Oliveros, C. Minguillón, J. Chromatogr. A 906 (2001) 155.
[7] B. Sellergren, J. Chromatogr. A 906 (2001) 227.
[8] J. Blehaut, R.-M. Nicoud, Anal. Mag. 26 (1998) M60.
[9] M. Kaspereit, P. Jandera, M. Skavrada, A. Seidel-Morgenstern, J. Chromatogr. A 944 (2002) 249.
[10] M. Kaspereit, H. Lorenz, A. Seidel-Morgenstern, in: K. Kaneko, et al. (Eds.), Fundamentals of Adsorption, vol. 7, IK International, Shinjuko, Japan, 2002, p. 101.
[11] H. Lorenz, P. Sheehan, A. Seidel-Morgenstern, J. Chromatogr. A 908 (2001) 201.
[12] B.-G. Lim, C.-B. Ching, R.B.H. Tan, S.-C. Ng, Chem. Eng. Sci. 50 (1995) 2289.
[13] B.-G. Lim, R.B.H. Tan, S.-C. Ng, C.-B. Ching, Chirality 7 (1995) 74.
[14] G. Ströhlein, M. Schulte, J. Strube, Sep. Sci. Technol. 38 (2003) 3353.
[15] J. Jacques, A. Collet, S.H. Wilen, Enantiomers, Racemates and Resolutions, Krieger, Malabar, 1994.
[16] P.R. Rony, Sep. Sci. 3 (1968) 239.
[17] M.F. Doherty, M.F. Malone, Conceptual Design of Distillation Systems, McGraw-Hill, New York, 2001, pp. 51–59.
[18] G. Guiochon, J. Chromatogr. A 965 (2002) 129.
[19] D.M. Ruthven, C.B. Ching, Chem. Eng. Sci. 44 (1989) 1011.
[20] M. Mazzotti, G. Storti, M. Morbidelli, J. Chromatogr. A 769 (1997) 3.
[21] C. Heuer, H. Kniep, T. Falk, A. Seidel-Morgenstern, Chem. Eng. Technol. 21 (1998) 469.
[22] P. Jandera, M. Skavrada, K. Klemmova, V. Backovska, G. Guiochon, J. Chromatogr. A 908 (2001) 19.
[23] A. Seidel-Morgenstern, J. Chromatogr. A 1037 (2004) 255.
[24] C. Blümel, P. Hugo, A. Seidel-Morgenstern, J. Chromatogr. A 865 (1999) 51.
[25] C.B. Ching, K.H. Chu, D.M. Ruthven, AIChE J. 36 (1990) 275.
[26] H. Lorenz, D. Sapoundjiev, A. Seidel-Morgenstern, J. Chem. Eng. Data 47 (2002) 1280.
[27] D. Sapoundjiev (MPI Magdeburg), unpublished data.
[28] G. Biressi, O. Ludemann-Hombourger, M. Mazzotti, R.-M. Nicoud, M. Morbidelli, J. Chromatogr. A 876 (2000) 3.
[29] F.G. Helfferich, J. Chromatogr. A 768 (1997) 169.
[30] Z. Zhang, M. Mazzotti, M. Morbidelli, J. Chromatogr. A 989 (2003) 95.
[31] M. Ginkel, A. Kremling, T. Nutsch, R. Rehner, E.D. Gilles, Bioinformatics 19 (2003) 1169.
[32] F. Tränkle, M. Zeitz, M. Ginkel, E.D. Gilles, Mathematical and computer modelling of dynamical systems 6 (2000) 283.
[33] The NAG Library, Mark 15, vols. 1–10, NAG Ltd., Oxford, 1991.
[34] A. Toumi, S. Engell, O. Ludemann-Hombourger, R.M. Nicoud, M. Bailly, J. Chromatogr. A 1006 (2003) 15.
[35] R.-M. Nicoud, in: G. Subramanian (Ed.), Bioseparation and Bioprocessing, vol. 1, VCH, Wiley, 1998, pp. 3–39.